Stability and structure of atomic chains on Si(111)

Corsin Battaglia* and Philipp Aebi
Institut de Physique, Université de Neuchâtel, 2000 Neuchâtel, Switzerland

Steven C. Erwin
Center for Computational Materials Science, Naval Research Laboratory, Washington DC 20375, USA
(Received 13 May 2008; revised manuscript received 13 June 2008; published 11 August 2008)

We study the stability and structure of self-assembled atomic chains on Si(111) induced by monovalent, divalent, and trivalent adsorbates, using first-principles total-energy calculations and scanning tunneling microscopy. We find that only structures containing exclusively silicon honeycomb or silicon Seiwatz chains are thermodynamically stable, while mixed configurations, with both honeycomb and Seiwatz chains, may be kinetically stable.

DOI: 10.1103/PhysRevB.78.075409 PACS number(s): 68.47.Fg, 81.16.Dn, 71.15.Mb, 68.37.Ef

I. INTRODUCTION

Understanding and controlling the structure of surfaces on the atomic level is of tremendous technological importance. This is especially true for the growth of semiconductor nanostructures, where the competition between thermodynamics and kinetics can play a decisive role. The reconstruction of semiconductor surfaces is driven by the elimination of dangling bonds and the minimization of surface stress, with a striking diversity of outcomes. Despite this variety, even very elaborate architectures are generally comprised of a small number of elementary structural building blocks. Dimers and adatoms on Si(100) and Si(111), respectively, are the best known strategies for reducing the number of dangling bonds. Tetramers and pentamers, encountered on Si(114),[1] Si(113),[2] Si(110),[3,4] and Si(331),[5] constitute more complex units. For adsorbate-induced surface reconstructions of the Si(111) surface, honeycomb[6–8] and Seiwatz chains[9] have recently emerged as universal building blocks[10] (see Fig. 1). These form the basis of a large class of atomic chain reconstructions which have been the focus of intense research because of their fascinating quasi-one-dimensional electronic properties.[11–16] The fact that only silicon atoms participate in the formation of the honeycomb and Seiwatz chains means that a number of different adsorbates can induce a chain reconstruction, simply by donating the correct number of electrons to the substrate.

We have recently revealed remarkable systematics in this class of adsorbate-induced reconstructions, relating the valence state of the adsorbate to the allowed coverages and periodicities of the resulting adsorbate chains.[10,17] All experimentally observed phases satisfy a simple electron-counting rule: The adsorbates must provide one electron to stabilize each (3×1) honeycomb-chain unit and two electrons to stabilize each (2×1) Seiwatz-chain unit.[8,10,18,19] For monovalent adsorbates[6–8] the only experimentally observed configuration is obtained with an adsorbate coverage of 1/3 monolayer (ML).[20] This corresponds to one adsorbate donating one electron per (3×1) honeycomb-chain unit as shown in Fig. 1(a), in agreement with the electron-counting rule. For divalent adsorbates, only 1/6 ML (half the monovalent adsorbate coverage) is required to stabilize honeycomb chains,[19,21–24] since a divalent adsorbate donates two electrons. The pure Seiwatz-chain structure shown in Fig. 1(b) is stable for 1/2 ML of divalent adsorbates,[25,26] resulting from two donated electrons per (2×1) Seiwatz-chain unit.[10] A mixed chain phase, alternating between honeycomb and Seiwatz chains as shown in Fig. 1(c), observed for divalent adsorbates[25,26] at intermediate coverage of 3/10 ML, also satisfies the electron-counting rule.[10] Here the divalent adsorbates supply one electron to the honeycomb-chain unit and two electrons to the Seiwatz-chain unit. Similarly, trivalent adsorbates at a coverage of 2/10 ML donate the same number of electrons, allowing the same mixed phase to be stabilized.[10]

In this report we subject these observed systematics, as well as the electron-counting rule deduced from them, to more detailed theoretical scrutiny. Specifically, we examine theoretically the thermodynamic and kinetic stability of several chain reconstructions of Si(111) by using first-principles total-energy methods. We compare the resulting pictures that emerge for three prototypical adsorbates: monovalent (Na), divalent (Ca), and trivalent (Gd). For each adsorbate we compare a number of reconstructions with different adsorbate coverages, including the bare Si(111)–(7×7) reconstruction, and for Ca and Gd adsorbates, the silicide phases

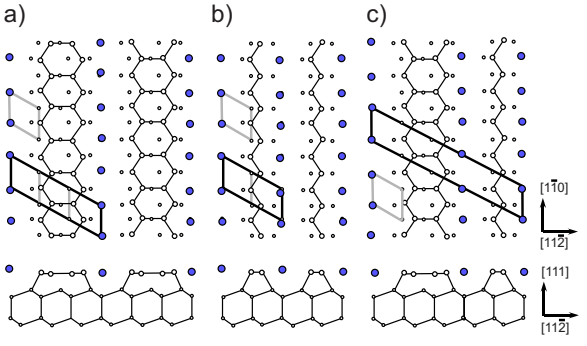

FIG. 1. (Color online) Top (upper) and side (bottom) views of the two prototypical silicon chains separated by channels that accommodate the adsorbate atoms [filled blue (gray) circles]. (a) Honeycomb chain with (3×1) unit cell. (b) Seiwatz chain with (2×1) unit cell. (c) Mixed chain structure with (5×1) unit cell. The (1×1) unit cell of the (111)-oriented substrate is indicated in gray. The crystallographic directions of the substrate are also indicated.

experimentally observed at higher coverage. For each candidate reconstruction, we determine the surface energy as a function of adsorbate chemical potential and thereby determine the energy ordering of our candidate reconstructions at any thermodynamically allowed value of chemical potential. We find that the thermodynamically stable chain reconstructions are formed exclusively from either honeycomb or Seiwatz chains, with mixed phases slightly higher in energy. We also argue that for Gd adsorbates the experimentally observed mixed phase, which combines honeycomb and Seiwatz chains, while not thermodynamically stable, is kinetically stable. This scenario is supported by experimental scanning tunneling microscopy (STM) data presented hereafter.

II. METHODS

We used first-principles total-energy calculations to determine equilibrium geometries and relative surface energies. The calculations were performed in a slab geometry with up to six layers of Si plus the reconstructed surface layer. All atomic positions were relaxed except for the bottom layer, which was passivated. Total energies and forces were calculated within the generalized-gradient approximation to density-functional theory (DFT), using projector-augmented-wave (PAW) potentials as implemented in VASP.[27,28] We checked that the slab thickness, plane-wave cutoff, and sampling of the surface Brillouin zone were each sufficient to converge the relative surface energies to within 1 meV/Å^2.[29]

For calculations with Gd adsorbates, the seven $4f$ electrons were treated explicitly as valence states.[30] The possibility of magnetic order among Gd atoms within a single fully occupied channel was investigated in one case, with the result that ferromagnetic ordering was slightly preferred, by 0.5 eV per Gd, to antiferromagnetic ordering. Based on this finding, we assumed ferromagnetic order for all Gd phases. We also found that putting the $4f$ electrons in the core led to only insignificant changes to the calculated absolute surface energies. This establishes that magnetic order among the Gd atoms plays no substantive role in the stability of different surface phases.

Growth and STM experiments were carried out in an ultrahigh vacuum chamber with a residual gas pressure of 3×10^{-11} mbar equipped with an Omicron LT STM. Boron-doped Si(111) with a resistivity of 5 Ω cm was heated by passing a direct current. Gd was evaporated from a water-cooled e-beam evaporator.

We consider first the stability of atomic chains induced by monovalent adsorbates such as the alkali metals Li, Na, K, Rb, and Cs. These are known to induce a chain reconstruction on Si(111) exhibiting simple (3×1) periodicity. The widely accepted structural model, the so-called honeycomb-chain-channel (HCC) model,[6–8] is shown in Fig. 1(a). The HCC model consists of Si honeycomb chains aligned along the $[1\bar{1}0]$ direction, separated by empty channels. The adsorbate atoms occupy sites within these channels.

The presence of an adsorbate, such as Na, in the HCC model does not allow direct comparison between its surface energy and the surface energy of clean reconstructed Si(111)$-(7\times7)$. The proper way to compare energies of structures differing in stoichiometry is via the chemical potentials μ_{Si} and μ_{Na} of the constituents,[31] which are the energy per atom available in the reservoirs with which the surface is assumed to be in equilibrium. The surface energy (per unit area) is then

$$\gamma = E_{\mathrm{surf}}/A = (E_{\mathrm{tot}} - n_{\mathrm{Si}}\mu_{\mathrm{Si}} - n_{\mathrm{Na}}\mu_{\mathrm{Na}})/A, \quad (1)$$

where E_{tot} is the total energy of a double-sided slab whose unit cell, with total area A, contains n_{Si} Si atoms and n_{Na} Na atoms. Since the surface is in equilibrium with the bulk Si substrate, μ_{Si} is the energy per atom in bulk Si. The adsorbate chemical potential μ_{Na}, however, corresponds to a real physical variable that can be externally tuned by, for example, varying the partial pressure of Na. Intuitively, increasing the Na partial pressure will increase the stability of structures with higher Na coverage. This is evident from recasting Eq. (1) as

$$\gamma = \gamma_0 - \theta_{\mathrm{Na}}\mu_{\mathrm{Na}}, \quad (2)$$

where θ_{Na} is the adsorbate coverage. From Eq. (2) it is clear that reconstructions with larger θ_{Na} are increasingly favored as μ_{Na} increases. For a given value of μ_{Na}, the reconstruction with the lowest surface energy γ will be realized in an experiment if it is performed under conditions of thermodynamic equilibrium. Phase transitions can thus occur as μ_{Na} is changed.

Thermodynamics places an upper bound on the adsorbate chemical potential, $\mu_{\mathrm{Na}} \leq \mu^0_{\mathrm{Na}}$, given by the energy per atom in the ground-state (body-centered-cubic) phase of elemental Na. Exceeding this limit in an experiment would result in precipitation of elemental Na because that phase would then be energetically preferable to any adsorbed phase. There is no lower bound on the adsorbate chemical potential because the only bulk phase with which the system must be in equilibrium is silicon. Hence by making the chemical potential sufficiently low (by turning the partial pressure to a very small value), the bare surface will be the most stable phase. The more interesting question is what happens in between these two extremes.

III. RESULTS AND DISCUSSION

A. Monovalent adsorbates

The calculated DFT surface energies, as a function of chemical potential, are shown in Fig. 2(a) for several reconstructions of Si(111) induced by the monovalent adsorbate Na. All surface energies are given relative to that of the bare Si(111)$-(7\times7)$, which we place at $\gamma=0$.[32] The colored lines with nonzero slopes represent the surface energies for various Na-induced reconstructions. Results for two HCC phases are shown (blue dashed lines), with $\theta_{\mathrm{Na}}=1/3$ and 1/6 ML, corresponding to fully occupied (3×1) and half-filled (3×2) channels, respectively. Also shown are results for two Seiwatz-chain phases (green dotted lines), with $\theta_{\mathrm{Na}}=1/2$ and 1/4 ML, corresponding to fully occupied (2×1) and half-filled (2×2) channels, respectively. Finally, results for

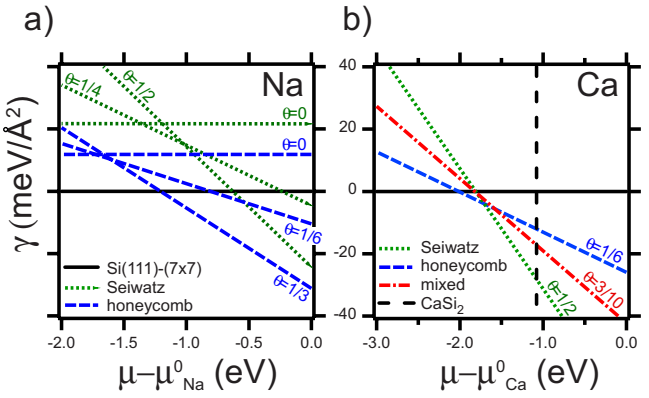

FIG. 2. (Color online) (a) Surface-energy diagram for monovalent Na adsorbates. We compare pure honeycomb chains ($\theta=1/3$, 1/6, and 0 ML; blue dashed lines) and pure Seiwatz chains ($\theta=1/2$, 1/4, and 0 ML; green dotted lines). The surface energy of Si(111)–(7×7) ($\theta=0$ ML, black line) is also shown. (b) Surface-energy diagram for divalent Ca adsorbates. We compare pure honeycomb chains ($\theta=1/6$, blue dashed line), pure Seiwatz chains ($\theta=1/2$, green dotted line), and a mixed chain configuration with alternating honeycomb and Seiwatz chains ($\theta=3/10$, red dotted-dashed line). The vertical dashed line represents the bulk $CaSi_2$ silicide.

"empty" HCC and Seiwatz reconstructions (i.e., without adsorbates) are shown as flat lines.

From the energy ordering of these various reconstructions, it is evident that over the allowed range of μ_{Na}, only two phases are thermodynamically stable: the clean Si(111)–(7×7) surface and the (3×1) HCC phase with $\theta_{Na}=1/3$, in agreement with experiment. We find, but do not show here, very similar results for other monovalent adsorbates (Li and K) and conclude that for monovalent adsorbates the only thermodynamically stable phase is the HCC with every site in the channel occupied.

B. Divalent adsorbates

We turn now to reconstructions induced by divalent adsorbates, such as the alkaline-earth metals (Mg, Ca, Sr, and Ba) and rare-earth metals (Sm, Eu, and Yb). From experiments we know that at a coverage of 1/6 ML, divalent adsorbates stabilize (3×"2") honeycomb chains.[33] At a coverage of 1/2 ML, the (2×1) Seiwatz chains are experimentally observed.[25,26] At intermediate coverages, divalent adsorbates are known to stabilize mixed chain structures with higher periodicity consisting of a combination of honeycomb chains and Seiwatz chains. The simplest combination alternates between honeycomb and Seiwatz chains, resulting in a (5×1) unit cell, as shown in Fig. 1(c). The (5×"2") periodicity observed for divalent adsorbates may be thought of as being built from two (3×1) honeycomb-chain units and two (2×1) Seiwatz-chain units.

We have calculated the surface energies of a variety of candidate reconstructions based on the divalent adsorbate Ca, including pure honeycomb chains with coverages $\theta=1/3$ and 1/6 ML, pure Seiwatz chains with coverages $\theta=1/2$ and 1/4 ML, and the mixed configuration alternating between honeycomb and Seiwatz chains with adsorbate coverages $\theta=2/10$, 3/10, and 4/10 ML. A new consideration arises for Ca because Si and Ca can form a variety of stable bulk silicides, such as $CaSi_2$ and Ca_2Si. To prevent precipitation of these bulk phases, the Ca and Si chemical potentials must also satisfy the inequalities

$$\mu_{Ca}+2\mu_{Si}\leq\mu(CaSi_2), \tag{3}$$

$$2\mu_{Ca}+\mu_{Si}\leq\mu(Ca_2Si), \tag{4}$$

where $\mu(CaSi_2)$ is the energy per formula unit of $CaSi_2$ and $\mu(Ca_2Si)$ is that for Ca_2Si. Since μ_{Si} is fixed, these constraints have the effect of further lowering the highest allowed value of μ_{Ca}.

The resulting surface energies for Ca-induced reconstructions are shown in Fig. 2(b). To keep the figure uncluttered, we have plotted only the phases that are stable, or close to stable, for some allowed value of μ_{Ca}. Two Ca-induced phases are thermodynamically stable: the HCC reconstruction with $\theta=1/6$ ML (blue dashed line) and the Seiwatz-chain reconstruction with $\theta=1/2$ ML (green dotted line). The mixed HCC+Seiwatz configuration with $\theta=3/10$ ML (red dotted-dashed line) is energetically just above these two phases. However, the minimum energy difference between these phases is so small (about 1 meV/Å^2) that we cannot draw any definitive prediction from it regarding the formation of the mixed configuration. Experimentally, the mixed configuration is indeed found at coverages between those of the two pure phases.

C. Trivalent adsorbates

Experiments using trivalent adsorbates (Gd, Dy, Er, and Ho) reveal a mixed configuration with (5×"2") periodicity consisting of alternating honeycomb and Seiwatz chains, as shown in Fig. 1(c). Pure honeycomb- or pure Seiwatz-chain structures are not observed. We have calculated the surface energies of a number of hypothetical Gd-induced configurations, including pure honeycomb chains with every channel site occupied ($\theta=1/3$ ML), every second site occupied ($\theta=1/6$ ML), and every third site occupied ($\theta=1/9$ ML), as well as of Seiwatz chains with every channel site occupied ($\theta=1/2$ ML) and every second site occupied ($\theta=1/4$ ML). We also considered three mixed configurations with $\theta=2/10$, 3/10, and 4/10 ML. Finally, we also calculated the surface energy for the well-studied epitaxial $GdSi_2$ silicide, which consists of 1 ML of Gd on Si(111) in the so-called B-T4 structure.[34,35]

The resulting surface energies for Gd-induced reconstructions are shown in Fig. 3(a). As before, we plot only the phases that are stable, or nearly so. There are two thermodynamically stable phases, the bare Si(111)–(7×7) and the $GdSi_2$ silicide phase with $\theta_{Gd}=1$. None of the Gd-chain reconstructions is thermodynamically stable within DFT.

To investigate the possibility that the experimentally observed phases are kinetically stable, we examine in detail the energetics of all phases with intermediate Gd coverage. In particular, we are interested in the tendency of an adsorbate phase with intermediate coverage θ_{Gd} to separate into two

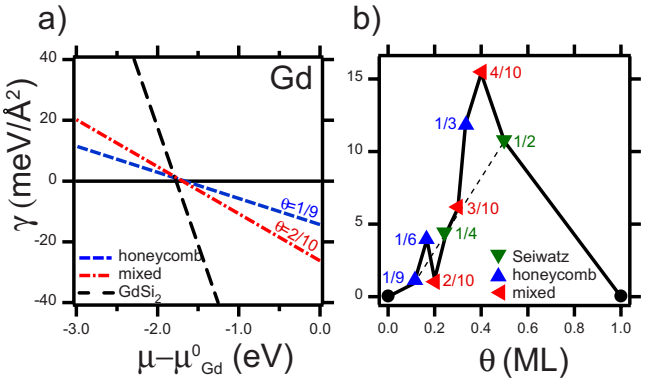

FIG. 3. (Color online) (a) Surface-energy diagram for the trivalent adsorbate Gd. We compare pure honeycomb chains ($\theta=1/9$, blue dashed line) and a mixed chain configuration with alternating honeycomb and Seiwatz chains ($\theta=2/10$, red dotted-dashed line). The horizontal line represents Si(111)$-(7\times7)$ ($\theta=0$ ML, black), and the black dashed line represents the $GdSi_2$ silicide film ($\theta=1$ ML). (b) Surface energies of Gd phases plotted as a function of coverage. Only the points have meaning; the lines are added for clarity.

stable phases, one with lower coverage θ_{Gd}^{-} and one with higher coverage θ_{Gd}^{+}. Let x denote the fraction of the total surface area occupied by the higher-coverage phase. Then the average coverage of the two phases is simply $x\theta_{Gd}^{+}+(1-x)\theta_{Gd}^{-}$. If x is chosen such that this average coverage is equal to the coverage θ_{Gd} of the homogeneous phase, then the surfaces energies of the homogeneous and inhomogeneous phases can be compared directly, without the need for specifying a chemical potential. To make this comparison simple, we return to Eq. (2) and now regard the surface energy γ as a function of coverage θ_{Gd} for a fixed, arbitrary value of chemical potential μ_{Gd}. Although the surface energies for the individual phases depend explicitly on μ_{Gd}, the energy difference between the two alternative scenarios (the homogeneous phase versus the phase-separated phase) with the same average coverage does not.

The resulting surface energies, for all the Gd-chain phases we have considered, are plotted in Fig. 3(b) relative to the two thermodynamically stable end-point phases [Si(111)$-(7\times7)$ and $GdSi_2$] as a function of Gd coverage. For display purposes we chose the value of the chemical potential for which the two end-point phases have equal surface energies. For intermediate Gd coverages, the surface energy is always higher than at the end points. Thus, a surface prepared with intermediate coverage will, under conditions of thermodynamic equilibrium, phase separate into an appropriate mixture of the two end-point phases. What about conditions under which thermodynamic equilibrium cannot be achieved?

There are good reasons to consider this scenario. The conversion of an intermediate phase to a combination of bare (7×7) and $GdSi_2$ silicide phases requires a considerable rearrangement of the top several atomic layers; this restructuring may be kinetically hindered. On the other hand, the structural differences among the various Gd-chain phases are relatively minor: For example, all are quasi-one-dimensional with similar underlying building blocks. Thus, the thermodynamically favored end-point phases may be kinetically inaccessible, even though equilibrium is achieved among the subset of structurally similar chain phases with intermediate coverage.

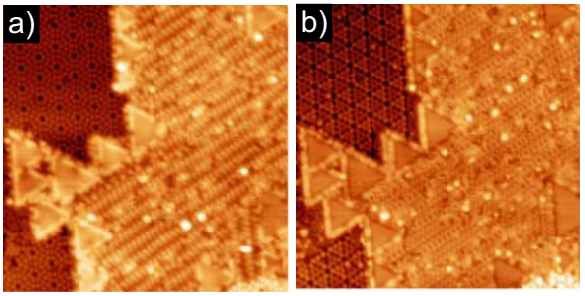

FIG. 4. (Color online) (a) Empty- and (b) filled-state STM images of Si(111) surface after Gd deposition and subsequent annealing. Atomic chains coexist with clean areas with the Si(111)$-(7\times7)$ reconstruction separated by triangular $GdSi_2$ islands. $U=\pm1.8$ V, $I=0.18$ nA, and 45×45 nm^2.

To support our hypothesis, we apply a geometrical analysis to the phases with intermediate Gd coverage, which allows one to find out if any of the intermediate phases is stable against phase separation into appropriate mixtures of all other intermediate phases. We consider again the results in Fig. 3(b) and construct a series of analogous plots (not shown), this time with the (7×7) and $GdSi_2$ end points excluded. Of the remaining phases, only one is stable with respect to phase separation into all possible intermediate-coverage end-point pairs: the (5×2) mixed HCC+Seiwatz phase with $\theta_{Gd}=2/10$. Geometrically, this conclusion is easy to visualize in Fig. 3(b) by simply drawing straight lines between all possible pairs of phases. The dotted line shows one such example, demonstrating the stability of the $\theta_{Gd}=2/10$ phase with respect to separation into the two end-point phases, with $\theta_{Gd}=1/9$ and $\theta_{Gd}=1/2$.

Further evidence for the kinetic scenario is obtained from our experimental observations. Starting with the deposition of 2/10 ML Gd onto the substrate held at 680 °C, followed by short annealing still at 680 °C and a cooldown to room temperature, one obtains a surface uniformly covered with atomic chains. After annealing for a slightly longer period or at slightly higher temperatures, phase separation may directly be observed in STM images (see Fig. 4): Triangles of $GdSi_2$ silicide form together with regions of clean Si(111)$-(7\times7)$ coexisting with the chains. Further annealing completely transforms the chains into silicide islands and areas with Si(111)$-(7\times7)$.

IV. CONCLUSION

We used first-principles total-energy calculations and scanning tunneling microscopy to study the stability and structure of atomic chains of monovalent, divalent, and trivalent adsorbates on Si(111). For monovalent adsorbates the theoretical and experimental results are in excellent agreement, both identifying the HCC reconstruction with adsorbate coverage $\theta=1/3$ as the only stable chain phase. For divalent adsorbates three chain phases are found experimen-

tally, corresponding to coverages of 1/6 and 1/2 and intermediate values. These findings are corroborated by our total-energy calculations, which identify the three lowest-energy phases as a half-occupied HCC phase, a fully occupied Seiwatz-chain phase, and a simple combination of these. For trivalent adsorbates, our total-energy calculations indicate that the observed combination of HCC and Seiwatz phases with adsorbate coverage of 2/10 is kinetically stable with respect to phase separation into other, thermodynamically more stable phases. For all adsorbates, the thermodynamically (or kinetically) stable phases all obey a surprisingly simple electron-counting rule proposed earlier.[10,17]

ACKNOWLEDGMENTS

We thank Franz J. Himpsel for stimulating discussions. The help of Leslie-Anne Fendt, Samuel Hoffmann, Claude Monney, and Christoph Walther is gratefully acknowledged. Skillful technical assistance was provided by our workshop and electric engineering team. This work was supported by the Fonds National Suisse pour la Recherche Scientifique through Division II, MaNEP, and the U.S. Office of Naval Research. Computations were performed at the DoD Major Shared Resource Center at ASC.

*corsin.battaglia@unine.ch; http://www.unine.ch/phys/spectro

[1] S. C. Erwin, A. A. Baski, and L. J. Whitman, Phys. Rev. Lett. **77**, 687 (1996).
[2] A. Laracuente, S. C. Erwin, and L. J. Whitman, Phys. Rev. Lett. **81**, 5177 (1998).
[3] T. An, M. Yoshimura, I. Ono, and K. Ueda, Phys. Rev. B **61**, 3006 (2000).
[4] A. A. Stekolnikov, J. Furthmüller, and F. Bechstedt, Phys. Rev. Lett. **93**, 136104 (2004).
[5] C. Battaglia, K. Gaál-Nagy, C. Didiot, C. Monney, E. F. Schwier, M. G. Garnier, and P. Aebi, arXiv:0807.3875.
[6] C. Collazo-Davila, D. Grozea, and L. D. Marks, Phys. Rev. Lett. **80**, 1678 (1998).
[7] L. Lottermoser *et al.*, Phys. Rev. Lett. **80**, 3980 (1998).
[8] S. C. Erwin and H. H. Weitering, Phys. Rev. Lett. **81**, 2296 (1998).
[9] R. Seiwatz, Surf. Sci. **2**, 473 (1964).
[10] C. Battaglia, H. Cercellier, C. Monney, M. G. Garnier, and P. Aebi, Europhys. Lett. **77**, 36003 (2007).
[11] J. N. Crain, A. Kirakosian, K. N. Altmann, C. Bromberger, S. C. Erwin, J. L. McChesney, J.-L. Lin, and F. J. Himpsel, Phys. Rev. Lett. **90**, 176805 (2003).
[12] T. Okuda, T. Tohyama, X.-D. Ma, T. Wakita, A. Harasawa, and T. Kinoshita, J. Electron Spectrosc. Relat. Phenom. **137-140**, 125 (2004).
[13] J. R. Ahn, P. G. Kang, K. D. Ryang, and H. W. Yeom, Phys. Rev. Lett. **95**, 196402 (2005).
[14] J. Guo, G. Lee, and E. W. Plummer, Phys. Rev. Lett. **95**, 046102 (2005).
[15] P. C. Snijders, S. Rogge, and H. H. Weitering, Phys. Rev. Lett. **96**, 076801 (2006).
[16] K. Sakamoto, P. E. J. Eriksson, A. Pick, N. Ueno, and R. I. G. Uhrberg, Phys. Rev. B **74**, 235311 (2006).
[17] C. Battaglia, H. Cercellier, C. Monney, L. Despont, M. G. Garnier, and P. Aebi, J. Phys.: Conf. Ser. **100**, 052078 (2008).
[18] M. D. Pashley, Phys. Rev. B **40**, 10481 (1989).
[19] G. Lee, S. Hong, H. Kim, D. Shin, J. Y. Koo, H. I. Lee, and Dae Won Moon, Phys. Rev. Lett. **87**, 056104 (2001).
[20] We define 1 ML as the atom density of the bulk-terminated Si(111) surface of 7.8×10^{14} cm^{-2}.
[21] T. Okuda, H. Ashima, H. Takeda, K.-S. An, A. Harasawa, and T. Kinoshita, Phys. Rev. B **64**, 165312 (2001).
[22] D. Petrovykh, K. Altmann, J. Lin, F. Himpsel, and F. Leibsle, Surf. Sci. **512**, 269 (2002).
[23] O. Gallus, T. Pillo, P. Starowicz, and Y. Baer, Europhys. Lett. **60**, 903 (2002).
[24] K. Sakamoto, W. Takeyama, H. M. Zhang, and R. I. G. Uhrberg, Phys. Rev. B **66**, 165319 (2002).
[25] A. A. Baski, S. C. Erwin, M. S. Turner, K. M. Jones, J. W. Dickinson, and J. A. Carlisle, Surf. Sci. **476**, 22 (2001).
[26] T. Sekiguchi, F. Shimoksoshi, T. Nagao, and S. Hasegawa, Surf. Sci. **493**, 148 (2001).
[27] G. Kresse and J. Hafner, Phys. Rev. B **47**, 558 (1993).
[28] G. Kresse and J. Furthmüller, Phys. Rev. B **54**, 11169 (1996).
[29] We used kinetic-energy cutoffs of 245 eV for all calculations with Li, Na, K, and Ca and 256 eV for calculations with Gd. To sample the surface Brillouin zone, we used Γ-centered meshes: 8×8 for 1×1 surface unit cells, 4×4 for 2×2 and 3×3 surface unit cells, 2×4 for 5×2 surface unit cells, and 2×4 for 3×2 surface unit cells.
[30] We tested the Gd PAW potential by computing the equilibrium lattice parameter, *c/a* ratio, and bulk modulus of bulk ferromagnetic Gd in its ground-state hcp crystal structure. The results (3.66 Å, 1.59, and 40.0 GPa) are in excellent agreement with experimental values (3.63 Å, 1.59, and 41.3 GPa) from Ref. 36.
[31] E. Kaxiras, Y. Bar-Yam, J. D. Joannopoulos, and K. C. Pandey, Phys. Rev. B **35**, 9625 (1987).
[32] The surface energy for the Si(111)–(7×7) reconstruction was determined by calculating the surface energy of the Pandey model (Ref. 37) for Si(111)–(2×1) and subtracting the published DFT energy difference of 60 meV per (1×1) unit cell (Ref. 38).
[33] The ×"2" notation stands for the ×2 periodicity along the adsorbate chains but with missing coherence between adjacent chains.
[34] C. Rogero, C. Koitzsch, M. E. González, P. Aebi, J. Cerdá, and J. A. Martin-Gago, Phys. Rev. B **69**, 045312 (2004).
[35] C. Bonet, I. M. Scott, D. J. Spence, T. J. Wood, T. C. Q. Noakes, P. Bailey, and S. P. Tear, Phys. Rev. B **72**, 165407 (2005).
[36] M. Heinemann and W. M. Temmerman, Phys. Rev. B **49**, 4348 (1994).
[37] K. C. Pandey, Phys. Rev. Lett. **47**, 1913 (1981).
[38] K. D. Brommer, M. Needels, B. E. Larson, and J. D. Joannopoulos, Phys. Rev. Lett. **68**, 1355 (1992).